Hermite Interpolation with Euclidean Pythagorean Hodograph Curves

Zbyněk Šír

Faculty of Mathematics and Physics, Charles University in Prague
Sokolovská 83, 186 75 Praha 8
zbynek.sir@mff.cuni.cz

Abstract. We describe various algorithms for Hermite interpolation with Pythagorean Hodograph curves in Euclidean space. In this procedure we apply complex numbers and quaternions

Keywords: Hemite interpolation, Pythagorean Hodograph curves, quaternions

1 Introduction

Pythagorean hodograph (PH) curves (see the survey [3] and the references cited therein), form a remarkable subclass of polynomial parametric curves. They have a piecewise polynomial arc length function and, in the planar case, rational offset curves. These curves provide an elegant solution of various difficult problems occurring in applications, in particular in the context of CNC (computer-numerical-control) machining.

Our paper is devoted to the Hermite interpolation by PH curves, which seems to the most promising among various methods for their construction. Since it is essentially a local construction, it results in a relatively reasonable system of nonlinear equations, which can be explicitly solved in certain cases. Other (global) methods lead typically to a huge system of nonlinear equation having unclear solvability condition. As an additional problem it is necessary to make a choice among a great number of solutions.

After recalling some basic facts about PH curves in Euclidean space we outline the basic algorithm about C^1 interpolation in the plane and our results about C^2 Hermite interpolation in Euclidean space in the context of other interpolation techniques. Finally we conclude the paper.

2 Euclidean H curves

In this section we summarize some basic properties of Pythagorean Hodograph curves in Euclidean space.

A Bézier curve is called *Pythagorean Hodograph (PH)* if the length of its tangent vector, taken in the appropriate metric, depends in a polynomial way on the parameter. In particular

- $\mathbf{p}(t) = [x(t), y(t)]$ is called *planar PH curve* if there exists a polynomial $\sigma(t)$ such that

$$x'(t)^2 + y'(t)^2 = \sigma^2(t), \tag{1}$$

- $\mathbf{p}(t) = [x(t), y(t), z(t)]$ is called a *spatial PH curve* if there exists a polynomial $\sigma(t)$ such that

$$x'(t)^2 + y'(t)^2 + z'(t)^2 = \sigma^2(t). \tag{2}$$

The degree of $\sigma(t)$ equals $n-1$, where n is the degree of the PH curve. The curve $\mathbf{h}(t) = [x'(t), y'(t)\{, z'(t)\}]$ is called the *hodograph* of $\mathbf{p}(t)$.

The planar polynomial curve $\mathbf{p}(t)$ can be identified with complex valued polynomial $\mathbf{p}(t) = x(t) + iy(t)$. The hodograph $\mathbf{h}(t) = x'(t) + iy'(t)$ then satisfy the equation (1) if and only if it is of the form $\mathbf{h}(t) = \mathbf{w}(t)^2$, where $\mathbf{w}(t) = v(t) + iw(t)$ is a complex valued polynomial called *preimage*, [2].

In a similar way, the spatial polynomial curve $\mathbf{p}(t)$ can be identified with pure–quaternion–valued polynomial $\mathbf{p}(t) = x(t)\mathbf{i} + y(t)\mathbf{j} + z(t)\mathbf{k}$. The hodograph $\mathbf{h}(t) = x'(t)\mathbf{i} + y'(t)\mathbf{j} + z'(t)\mathbf{k}$ then satisfy the equation (2) if and only if it is of the form $\mathbf{h}(t) = \mathcal{A}(t)\,\mathbf{i}\,\mathcal{A}^*(t)$, where $\mathcal{A}(t) = u(t) + v(t)\mathbf{i} + p(t)\mathbf{j} + q(t)\mathbf{k}$ is a quaternion valued polynomial called *preimage*, [1].

In the Hermite interpolation one wants to construct a suitable object (a PH curve in our case) matching prescribed boundary data. This data are typically the end point positions and some additional constraints, which can be analytical (derivative vectors) or geometrical (tangent directions, curvature, etc.) information. In the former case we talk about C-interpolation, in the latter about G-interpolation.

3 C^1 Hermite interpolation by PH quintics

The following algorithm is based on results from [13].

Algorithm 1 *Procedure* `PHQuintic`$(\mathbf{P}_0, \mathbf{V}_0, \mathbf{P}_1, \mathbf{V}_1)$
Input: *End points* $\mathbf{P}_0$, $\mathbf{P}_1$ *and end point derivatives (velocity vectors)* $\mathbf{V}_0$, $\mathbf{V}_1$. *All these data are considered as complex numbers, by identifying the plane with the Argand diagram.*
Output: *PH quintic* $\mathbf{p}(\tau)$ *defined over the interval* $[0,1]$ *and interpolating the input.*

1. *Transform the data to a certain canonical position,*

$$\tilde{\mathbf{V}}_0 = \frac{\mathbf{V}_0}{\mathbf{P}_1 - \mathbf{P}_0}, \qquad \tilde{\mathbf{V}}_1 = \frac{\mathbf{V}_1}{\mathbf{P}_1 - \mathbf{P}_0}.$$

2. *Compute the control points of the so–called preimage:*

$$\mathbf{w}_0 = \sqrt[+]{\tilde{\mathbf{V}}_0}, \qquad \mathbf{w}_2 = \sqrt[+]{\tilde{\mathbf{V}}_1}.$$

$$\mathbf{w}_1 = \frac{-3(\mathbf{w}_0 + \mathbf{w}_2) + \sqrt[+]{120 - 15(\tilde{\mathbf{V}}_0 + \tilde{\mathbf{V}}_1) + 10\mathbf{w}_0\mathbf{w}_2}}{4},$$

where $\sqrt[+]{}$ *denotes square root with the positive real part.*

3. *Compute the control points of the hodograph (i.e., the first derivative vector) and transform it back to the original position:*

$$\begin{aligned}
\mathbf{h}_0 &= \mathbf{w}_0^2(\mathbf{P}_1 - \mathbf{P}_0) \\
\mathbf{h}_1 &= \mathbf{w}_0\mathbf{w}_1(\mathbf{P}_1 - \mathbf{P}_0) \\
\mathbf{h}_2 &= (\frac{2}{3}\mathbf{w}_1^2 + \frac{1}{3}\mathbf{w}_0\mathbf{w}_2)(\mathbf{P}_1 - \mathbf{P}_0) \\
\mathbf{h}_3 &= \mathbf{w}_1\mathbf{w}_3(\mathbf{P}_1 - \mathbf{P}_0) \\
\mathbf{h}_4 &= \mathbf{w}_2^2(\mathbf{P}_1 - \mathbf{P}_0).
\end{aligned}$$

4. *Compute the control points of the PH interpolant,*

$$\mathbf{p}_0 = \mathbf{P}_0, \quad \mathbf{p}_i = \mathbf{p}_{i-1} + \frac{1}{5}\mathbf{h}_{i-1} \textit{ for } i = 1\ldots 5,$$

and return the PH curve in Bernstein-Bézier representation

$$\mathbf{p}(\tau) = \sum_{i=0}^{5} \mathbf{p}_i \binom{5}{i} \tau^i (1-\tau)^{5-i}.$$

Remark 1 It can be verified by a direct computation that the curve $\mathbf{p}(\tau)$ interpolates the input data and that it is a PH curve, i.e., its parametric speed is a (possibly piecewise) polynomial:

$$||\mathbf{p}'(\tau)|| = ||\mathbf{w}(\tau)||^2|\mathbf{P}_1 - \mathbf{P}_0|,$$

where

$$\mathbf{w}(\tau) = \mathbf{w}_0(1-\tau)^2 + 2\mathbf{w}_1\tau(1-\tau) + \mathbf{w}_2\tau^2$$

is the so–called preimage.

Remark 2 Algorithm `PHQuintic` fails for some rare cases of singular data. First of all the start point $\mathbf{P}_0$ and the end point $\mathbf{P}_1$ must be different because of the division in the step 1. Next, the function $\sqrt[+]{\ }$ is not defined on the line $\mathbb{R}_0^- = \{\lambda + 0\mathbf{i} : \lambda \in (-\infty, 0]\}$. In order to compute $\mathbf{w}_0$ and $\mathbf{w}_2$ it is therefore necessary that the input tangent vectors $\mathbf{V}_0$ and $\mathbf{V}_1$ are non-zero and that they are not opposite to the difference vector $\mathbf{P}_1 - \mathbf{P}_0$. Finally, we need

$$120 - 15(\tilde{\mathbf{V}}_0 + \tilde{\mathbf{V}}_1) + 10\mathbf{w}_0\mathbf{w}_2 \notin \mathbb{R}_0^-. \tag{3}$$

Note, that the vector $\mathbf{w}_0\mathbf{w}_2 = \sqrt[+]{\tilde{\mathbf{V}}_0\tilde{\mathbf{V}}_1}$ bisects the angle between $\tilde{\mathbf{V}}_0$ and $\tilde{\mathbf{V}}_1$ and its length is equal to the geometric average of the lengths of $\tilde{\mathbf{V}}_0$ and $\tilde{\mathbf{V}}_1$. Only input tangent vectors having a certain rare symmetry with respect to the difference vector $\mathbf{P}_1 - \mathbf{P}_0$ and at the same time being much longer $\mathbf{P}_1 - \mathbf{P}_0$ may violate condition (3). Various sufficient conditions can be determined for practical purposes in order to satisfy (3), e.g.,

$$||\mathbf{V}_i|| \leq 3||\mathbf{P}_1 - \mathbf{P}_0||, \quad i = 0, 1.$$

4 C^2 Hermite interpolation in plane and space

Table 1 summarizes the known results about Hermite interpolation in the Euclidean plane and space. One can observe two facts. First, interpolation of geometrical data is in principle more complicated then that of analytical data. Only the G^1 construction is available both in space and plane. The combined $G^2[C^1]$ interpolation in plane leads to the most complicated (quartic) equations. Moreover, while the C-interpolation has always a solution, this is not the case for G-interpolation, where certain conditions of solvability exist. Second, the space yields more freedom to satisfy the PH condition and therefore there are more interpolants of the same degree than in the plane.

Recently we gave new results concerning C^2 Hermite interpolation [14] and [15]. The task is to construct a PH curve $\mathbf{p}(t)$ matching given C^2 Hermite boundary data: the end points $\mathbf{p}_b$, $\mathbf{p}_e$, the first derivative vectors (velocities) $\mathbf{v}_b$, $\mathbf{v}_e$ and the second derivative vectors (accelerations) $\mathbf{a}_b$, $\mathbf{a}_e$. This can be done most efficiently by constructing the preimage. If we work in a suitable polynomial basis (such as Bernstein Bézier basis), the boundary condition which are linear for the curve $\mathbf{p}(t)$ and its hodograph $\mathbf{h}(t)$ become non-linear for the preimage $\mathbf{w}(t)$ or $\mathcal{A}(t)$. The resulting system can be however reduced to successive explicit solution (in quaternions or complex numbers) of several equations which are quadratic or linear (see Table 2).

While the complex number equation have a finite number of solution, the quaternion ones have one dimensional systems of solutions. We thus obtain a finite number of preimages for the planar case and multidimensional system of preimages in the space case. After eliminating some redundancies we finally obtain four PH interpolants in the planar case and a four dimensional system of solutions in the space case. Via an asymptotical analysis we were able to identify the "best" solution, which behaves in a most suitable way, when we interpolate data taken from an analytical curve and we diminish the step size.

As an example, Figure 1, left shows the system of spatial PH interpolants of degree 9 to the data

$$\begin{array}{lllllllll} \mathbf{p}_b & = & [0,0,0], & \mathbf{v}_b & = & [3,0,0], & \mathbf{a}_b & = & [0,1,0] \\ \mathbf{p}_e & = & [1,1,0], & \mathbf{v}_e & = & [3,0,0], & \mathbf{a}_e & = & [0,-1,0]. \end{array} \quad (4)$$

Note that these data lie in fact in the xy-plane and therefore the four dimensional system of spatial interpolants must contain the four planar interpolants (shown on the right figure).

5 Conclusion

The described constructions represent the state of art of the Hermite interpolation by PH curves. We were able to obtain construction methods

data	number of solutions	available results
	2D-plane	
G^1	2 solutions, quadratic equation (Walton and Meek [12])	One of the solutions has approximation order 4 at generic points [12].
C^1	4 solutions, quadratic equations (Farouki and Neff [6])	The best solution can be identified via its rotation index (Moon et al. [13]).
$G^2[C^1]$	8 solutions, quartic equations (Jüttler [9])	One of the solutions has approximation order 6 at generic points [9]. Inflections reduce the approximation order.
C^2	4 solutions, quadratic equations (Farouki et al. [5])	One of the solutions has approximation order 6 at all points (Šír and Jüttler [14]).
	3D-space	
G^1	2 solutions, quadratic equation (Jüttler and Mäurer [10])	One of the solutions has approximation order 4 at generic points (Mäurer and Jüttler [11]).
C^1	2–parametric system of solutions, quadratic equations in quaternions (Farouki and Neff [4])	One solution has the best approximation order 4, preserves planarity and symmetry of the data (Šír and Jüttler [16]).
C^2	4–parametric system of solutions, quadratic and linear equations in quaternions (Šír and Jüttler [15])	One solution has the best approximation order 6, preserves planarity and symmetry of the data [15].

Table 1: Hermite interpolation by Euclidean PH curves.

	2D-plane, comp. num.		3D-space, quater.	
	Equation	#Solutions	Equation	#Solutions
quadratic	$\mathbf{x}^2 = \mathbf{a}$	2	$\mathcal{X}\mathbf{i}\mathcal{X}^* = \mathcal{A}$	1-param. sys.
linear	$\mathbf{x}\mathbf{b} = \mathbf{a}$	1	$\mathcal{X}\mathcal{B} = \mathcal{A}$	1-param. sys.

Table 2: Two types of equation occurring in the C^2 Hermite interpolation process. The unknowns are $\mathbf{x}$ (complex number) or $\mathcal{X}$ (quaternion).

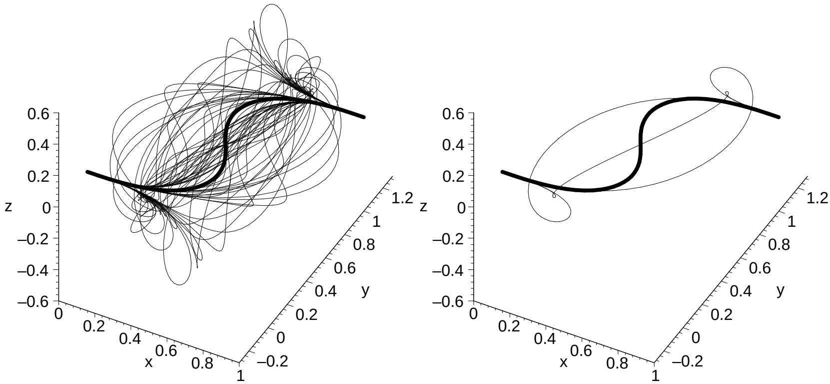

Figure 1: Left figure shows 64 representants of the four dimensional system of PH interpolants of the data (4). Right figure shows 4 interpolants, which are planar. The "best" interpolant is plotted in bold.

along with an analysis of the quality of the solutions. In this way we described the solution which can be used for example for conversion of analytical curves into PH splines or (in the Euclidean case) for smoothing tool paths.

Acknowledgment.

Zbyněk Šír was supported by the project MSM 0021620839 of the Czech Ministry of Education and by the project no. 201/08/0486 of the Czech Science Foundation.

References

[1] H.I. Choi, D.S. Lee & H.P. Moon (2002), Clifford algebra, spin representation, and rational parameterization of curves and surfaces. Adv. Comput. Math. 17, 5–48.

[2] R.T. Farouki (1994), The conformal map $z \to z^2$ of the hodograph plane. Comp. Aided Geom. Design 11, 363–390.

[3] R.T. Farouki (2002), Pythagorean–hodograph curves, Handbook of Computer Aided Geometric Design (J. Hoschek, G. Farin & M.-S. Kim, eds.), Elsevier, 405–427.

[4] R.T. Farouki, M. al-Kandari & T. Sakkalis (2002), Hermite interpolation by rotation-invariant spatial Pythagorean-hodograph curves., Adv. Comput. Math. 17, 369–383.

[5] R.T. Farouki, J. Manjunathaiah & S. Jee (1998), Design of rational cam profiles with Pythagorean-hodograph curves. Mech. Mach. Theory 33, 669–682.

[6] R.T. Farouki & C.A. Neff (1995), Hermite interpolation by Pythagorean-hodograph quintics, Math. Comput. 64, 1589–1609.
[7] R.T. Farouki & Sakkalis T. (1990), Pythagorean hodographs, IBM Journal of Research and Development, 34, 736–752.
[8] R.T. Farouki & T. Sakkalis (1994), Pythagorean-hodograph space curves, Adv. Comput. Math. 2, 41–66.
[9] B. Jüttler (2001), Hermite interpolation by Pythagorean hodograph curves of degree seven. Math. Comp. 70, 1089–1111.
[10] B. Jüttler & C. Mäurer (1999), Cubic Pythagorean Hodograph Spline Curves and Applications to Sweep Surface Modeling, Comp.–Aided Design 31, 73–83.
[11] C. Mäurer & B. Jüttler (1999), Rational approximation of rotation minimizing frames using Pythagorean–hodograph cubics, Journal for
[12] D.S. Meek & D.J. Walton (1997), Geometric Hermite interpolation with Tschirnhausen cubics, Journal of Computational and Applied Mathematics 81, 299–309.
[13] H.P. Moon, R.T. Farouki & H.I. Choi (2001), Construction and shape analysis of PH quintic Hermite interpolants, Comp. Aided Geom. Design 18, 93–115.
[14] Z. Šír & B. Jüttler (2004), Constructing acceleration continuous tool paths using pythagorean hodograph curves. Mech. Mach. Theory, 40(11):1258-1272, 2005.
[15] Z. Šír & B. Jüttler (2005), C^2 Hermite interpolation by space Pythagorean Hodograph curves, Math. Comp., 76(259):1373-1391, 2007.
[16] Z. Šír & B. Jüttler (2005), Spatial Pythagorean Hodograph Quintics and the Approximation of Pipe Surfaces, In R. Martin, H. Bez and M. Sabin, editors, The Mathematics of Surfaces XI, pages 364-380. Springer, 2005.